



HHS Public Access

Author manuscript

Neuroimage. Author manuscript; available in PMC 2021 January 25.

Published in final edited form as:

Neuroimage. 2021 January 15; 225: 117522. doi:10.1016/j.neuroimage.2020.117522.

Dynamic brain fluctuations outperform connectivity measures and mirror pathophysiological profiles across dementia subtypes: A multicenter study

Sebastian Moguilner^{a,b}, Adolfo M. García^{a,c,d,e}, Yonatan Sanz Per^{c,d,f}, Enzo Tagliazucchi^{c,f}, Olivier Piguet^g, Fiona Kumfor^g, Pablo Reyes^h, Diana Matallana^h, Lucas Sedeño^{c,*}, Agustín Ibáñez^{a,c,d,i,j,*}

^aGlobal Brain Health Institute (GBHI), University of California San Francisco (UCSF), California, US; & Trinity College Dublin, Dublin, Ireland ^bFundación Escuela de Medicina Nuclear (FUESMEN) and Comisión Nacional de Energía Atómica (CNEA), Buenos Aires, Argentina ^cNational Scientific and Technical Research Council (CONICET), Buenos Aires, Argentina ^dUniversidad de San Andrés, Buenos Aires, Argentina ^eFaculty of Education, National University of Cuyo (UNCuyo), Mendoza, Argentina ^fDepartment of Physics, University of Buenos Aires, Argentina ^gSchool of Psychology and Brain and Mind Centre, The University of Sydney, Sydney, Australia ^hMedical School, Aging Institute, Psychiatry and Mental Health, Pontificia Universidad Javeriana; Mental Health Unit, Hospital Universitario Fundación Santa Fe, Bogotá, Colombia, Hospital Universitario San Ignacio, Bogotá, Colombia ⁱUniversidad Autónoma del Caribe, Barranquilla, Colombia ^jCenter for Social and Cognitive Neuroscience (CSCN), School of Psychology, Universidad Adolfo Ibáñez, Santiago de Chile, Chile

Abstract

From molecular mechanisms to global brain networks, atypical fluctuations are the hallmark of neurodegeneration. Yet, traditional fMRI research on resting-state networks (RSNs) has favored static and average connectivity methods, which by overlooking the fluctuation dynamics triggered by neurodegeneration, have yielded inconsistent results. The present multicenter study introduces a data-driven machine learning pipeline based on dynamic connectivity fluctuation analysis (DCFA) on RS-fMRI data from 300 participants belonging to three groups: behavioral variant

This is an open access article under the CC BY-NC-ND license (<http://creativecommons.org/licenses/by-nc-nd/4.0/>)

*Corresponding authors. lucas.sedeno@gmail.com (L. Sedeño), agustin.ibanez@gbhi.org (A. Ibáñez).

Author contributions

Conception (AI, LS, and SM), design (SM and LS), acquisition and preprocessing (all), analysis (SM and LS), interpretation (AI, LS), draft manuscript (SM, LS, AI, AMG), substantial manuscript revision (all).

Data and code availability statement

The individual data from this study cannot be shared because of privacy issues of clinical data. Data from the datasets are available for research only after ethical approval for a specific project. Online datasets are available on their own online repositories [Alzheimer's Disease Neuroimaging Initiative (ADNI); and Neuroimaging In Frontotemporal Dementia (NIFD/LONI)]. The code for the data analysis of this study is available from the corresponding author on reasonable request.

Declaration of Competing Interest

The authors report no competing interests.

Supplementary materials

Supplementary material associated with this article can be found, in the online version, at doi:10.1016/j.neuroimage.2020.117522.

frontotemporal dementia (bvFTD) patients, Alzheimer's disease (AD) patients, and healthy controls. We considered non-linear oscillatory patterns across combined and individual resting-state networks (RSNs), namely: the salience network (SN), mostly affected in bvFTD; the default mode network (DMN), mostly affected in AD; the executive network (EN), partially compromised in both conditions; the motor network (MN); and the visual network (VN). These RSNs were entered as features for dementia classification using a recent robust machine learning approach (a Bayesian hyperparameter tuned Gradient Boosting Machines (GBM) algorithm), across four independent datasets with different MR scanners and recording parameters. The machine learning classification accuracy analysis revealed a systematic and unique tailored architecture of RSN disruption. The classification accuracy ranking showed that the most affected networks for bvFTD were the SN + EN network pair (mean accuracy = 86.43%, AUC = 0.91, sensitivity = 86.45%, specificity = 87.54%); for AD, the DMN + EN network pair (mean accuracy = 86.63%, AUC = 0.89, sensitivity = 88.37%, specificity = 84.62%); and for the bvFTD vs. AD classification, the DMN + SN network pair (mean accuracy = 82.67%, AUC = 0.86, sensitivity = 81.27%, specificity = 83.01%). Moreover, the DFCA classification systematically outperformed canonical connectivity approaches (including both static and linear dynamic connectivity). Our findings suggest that non-linear dynamical fluctuations surpass two traditional seed-based functional connectivity approaches and provide a pathophysiological characterization of global brain networks in neurodegenerative conditions (AD and bvFTD) across multicenter data.

Keywords

Dynamic functional connectivity; AD; bvFTD; fMRI resting-state connectivity; Copula-based dependence measure

1. Introduction

From molecular mechanisms to global networks, variable brain fluctuations are the hallmark of neurodegeneration. RSNs can be understood as dynamical systems presenting time-dependent functional connectivity (FC) variations that influence brain function during health and disease (Breakspear, 2017; Sporns, 2014; Hutchison et al., 2013). Despite this highly variable environment, most RSN research on dementia only employs static FC (SFC) measures (i.e., averages of FC across the whole MR acquisition time) (Sporns, 2014). Also, the field has broadly favored linear correlation measures (e.g., Pearson's R), which are blind to non-linear connectivity interactions. These limitations may partly explain why standard SFC analyses have yielded inconsistent sensitivity and specificity indices (Pievani et al., 2014; Sedeño, 2017) in classifying between Alzheimer's disease (AD) and behavioral variant frontotemporal dementia (bvFTD) patient groups (Pievani et al., 2014). The heterogeneous network fluctuations caused by neurodegeneration might not be captured by SFC and linear correlations, calling for non-linear FC methods and dynamical frameworks that outperform time-averaged connectivity (Liegeois et al., 2019). Here, we developed a Dynamic Connectivity Fluctuation Analysis (DCFA) which targets FC fluctuation across time and captures both linear and non-linear signal modulations (Fig. 1). We tested this framework's accuracy and generalizability to discriminate among healthy controls and two

dementia subtypes (AD and bvFTD), based on 300 subjects (from three international dementia centers and online databases).

Dementia involves a world-wide health-system burden, with an increasing prevalence and incidence in the US and other high-income countries (Wu et al., 2017) as well as in low- and middle-income countries (LMIC) (Wu et al., 2017; Kalaria et al., 2008, 9; Parra et al., 2018; Ibanez and Kosik, 2020). Moreover, the neuropathology of neurodegenerative disorders may manifest differences due to varied social, cultural, and regional contexts (Alladi and Hachinski, 2018). Functional network variability (Whitwell et al., 2009; Noh et al., 2014; Ossenkoppele et al., 2015), together with socioeconomic disparities, may induce heterogeneous presentations of AD and bvFTD, thus requiring robust approaches for its accurate characterization across heterogeneous populations. Such variability may in part explain conflicting evidence pointing to the most affected functional networks for each disease. Whereas some studies have reported that the Default Mode Network (DMN) and the Salience Network (SN) are differentially affected in AD and bvFTD, respectively (Pievani et al., 2014), others show aberrant FC along those networks in both conditions (Agosta et al., 2012; Filippi et al., 2019). Moreover, other networks, such as the EN, may also be disrupted in both dementia subtypes (Agosta et al., 2012; Badhwar et al., 2017). Therefore, there is a call for novel approaches that prove robust to sample heterogeneity.

Typical resting-state FC research assumes time-constant cross-regional interaction, establishing connectivity patterns as single association coefficients between the entire time-series while ignoring temporal variations (Hutchison et al., 2013). Despite the undeniable contribution of this approach (Hutchison et al., 2013), increasing evidence suggests that dynamic FC (DFC) changes may add critical information about brain organization (Breakspear, 2017; Hutchison et al., 2013), at different time scales and frequencies (Chang and Glover, 2010; Yaesoubi et al., 2015). Indeed, FC variability reflects task demands (Fornito et al., 2015), learning (Bassett et al., 2011), working memory (Shakil et al., 2016), and different consciousness states (Greicius et al., 2008). Dynamical fluctuations are related to specific electrophysiological bands, supporting their neurobiological relevance (Tagliazucchi et al., 2012). These changes are traceable at the typical temporal resolution of fMRI, as well as other (faster or slower) time-scales (from seconds to minutes) (Handwerker et al., 2012). Therefore, FC fluctuations seem critical to form adaptive activity patterns across different time-scales (Hutchison et al., 2013). This could underlie the cognitive and behavioral flexibility required to tackle environmental demands –which can hardly be captured by studying encapsulated mechanisms rooted in fixed functional architectures (Hutchison et al., 2013).

The DFC technique proved sensitive to neurological alterations indexed by FC changes over short periods, usually considering segmented time-windows (Shakil et al., 2016; Bolton et al., 2020). Most existing studies have investigated AD or Parkinson's disease (PD) (Hutchison et al., 2013), with only one reporting reduced DFC in FTD (Premi et al., 2019). Previous AD research has shown alterations in the DFC of the DMN-prefrontal cortex and in global oscillatory FC patterns (Filippi et al., 2019) correlated with cognitive symptom severity (Demirtas et al., 2017). Moreover, whereas a standard SFC approach discriminated early mild-cognitive impairment patients from controls with 62–72% accuracy, DFC yielded

a higher classification rate (80%) (Wee et al., 2016). Yet, this evidence presents several limitations. First, most of these studies (and others based on SFC approaches) overlook the combination of different RSNs as features to discriminate among dementias. Although the DMN and the SN are considered key altered networks in AD and bvFTD, respectively (Pievani et al., 2014), both present aberrant FC patterns in each disease (Agosta et al., 2012; Filippi et al., 2019). Moreover, other networks, such as the EN, have also been reported as impaired in these conditions (Agosta et al., 2012; Badhwar et al., 2017). Second, FC associations are generally estimated with linear metrics such as Pearson's correlations, despite substantial evidence highlighting the relevance of non-linear FC (Moguilner et al., 2018). Finally, the reliability and reproducibility of DFC findings remains a challenge given the lack of multicenter studies using computational decision-support methods, a robust framework to identify consistent biomarkers across countries (Humpel, 2011).

Against this background, we developed a novel DCFA framework and tested whether features based on connectivity fluctuations discriminate between AD and bvFTD across countries. Innovatively, this approach estimates interregional FC variability with a metric that captures both linear and non-linear associations, outperforming traditional seed-based functional connectivity metrics to characterize dementia (Moguilner et al., 2018). To evaluate the robustness of our pipeline, we employed an advanced machine-learning algorithm, the gradient boosting machines (GBM) (tuned by Bayesian hyperparameter optimization), with large training and test sets comprising 300 subjects from three international dementia centers and online databases. This allows testing the generalizability of our results, which proves critical for developing timely, cost-effective, and robust biomarkers (Sedeño, 2017). Moreover, unlike previous research, our approach allows assessing whether global brain dynamics (i.e., combinations between RSNs) proves more informative than single-network features. Considering the evidence above, we predicted that our DCFA pipeline would outperform SFC and linear DFC models in characterizing patients across centers. Furthermore, we hypothesized that models that factor in the combinations between fluctuations of two RSNs would outperform those targeting each network separately. In particular, in light of previous findings, we hypothesized that the combinations between the SN, the DMN, and the EN would be crucial to classify between bvFTD and AD patients, and also between the latter two groups and healthy controls. Lastly, as a complementary multimodal evaluation, we performed a one-sample comparison of DCFA and SFC relative to traditional anatomical MRI measures (surface-based morphometry, SBM).

2. Materials and methods

2.1. Participants

The study comprised 300 participants, with 150 individuals from our ongoing protocol (Donnelly-Kehoe et al., 2019; Baez et al., 2019; Sedeño et al., 2017; Santamaria-Garcia et al., 2017; Dottori et al., 2017; Sedeño et al., 2016; Melloni et al., 2016; Baez, 2016; Baez et al., 2014; Garcia-Cordero et al., 2019; Bachli, 2020) from three international clinical centers, and the remaining 150 belonging to the Alzheimer's Disease Neuroimaging Initiative (ADNI) and the Neuroimaging in Frontotemporal Dementia (NIFD/LONI)

databases, jointly referred as “online database ” below. Following recommendations for multicenter MRI studies (Poldrack et al., 2017), the set group of participants consisted of 51 healthy controls, 46 patients fulfilling revised criteria for probable bvFTD, and 53 with probable Alzheimer’s disease (AD), all recruited from centers with extensive experience in neurodegeneration: INECO Foundation, in Argentina (Country-1: 19 controls, 18 bvFTD patients, 15 CE patients); San Ignacio University Hospital, in Colombia (Country-2: 18 controls, 15 bvFTD patients, 20 AD patients); and the frontotemporal dementia research group (FRONTIER) at the University of Sydney, in Australia (Country-3: 14 controls, 13 bvFTD patients, 18 AD patients); and an online database (50 controls, 50 bvFTD patients, 50 AD patients).

As in previous reports (Sedeño et al., 2017; Baez et al., 2014; Piguet et al., 2011; Melloni et al., 2016), clinical diagnosis was established by bvFTD and AD expert clinicians and supported by a standard clinical examination including extensive neurological, neuropsychiatric, and neuropsychological assessments (Supplementary information 1). Then, each case was reviewed in a multidisciplinary clinical meeting involving cognitive/behavioral neurologists, psychiatrists, and neuropsychologists. The patients were impaired (i.e. in episodic memory for AD and prominent changes in personality and social behavior for bvFTD), as reported by caregivers. They were all in early/mild disease stages and did not fulfill criteria for specific psychiatric disorders. Patients presenting primarily with language deficits were excluded.

Patients from each group in each sample were matched on sex, age, and education with controls (Supplementary Table 1). No participant presented a history of drug abuse, and patients did not present other psychiatric or neurological diseases. All subjects provided signed informed consent in accordance with the Declaration of Helsinki. The study protocol was approved by each center’s institutional Ethics Committee.

2.2. Image acquisition

MRI acquisition and preprocessing steps followed the Organization for Human Brain Mapping guidelines (Poldrack et al., 2017) (Supplementary information 2). In the resting-state protocol, participants were asked not to think about anything in particular, while remaining awake, still and with eyes closed (Sedeño et al., 2017; Melloni et al., 2016). As in previous multicenter research (Sedeño et al., 2017; Moguilner et al., 2018; Donnelly-Kehoe, 2019; Dottori et al., 2017; Bachli et al., 2020), different scanners were used across centers, with diverse acquisition parameters (Supplementary Table 2). This variability is one of the strengths of multicenter approaches (Humpel, 2011), as it allows evaluating whether the same measure and machine-learning algorithm are sufficiently robust and reliable to discriminate among patients and controls despite methodological and sociocultural heterogeneity.

2.3. fMRI data preprocessing

For each preprocessing step, DPARSF called the Statistical Parametric Mapping (SPM 12) and the Resting-State fMRI Data Analysis Toolkit (REST V.1.7) to process the data. Before preprocessing, the first five volumes of each subject’s resting-state session were discarded to

ensure steady state magnetization. Then, the images were slice-time corrected (using as reference the middle slice of each volume) and aligned to the first scan of the session to correct head movement. To reduce the effects of motion and physiological artifacts, six head-motion parameters, as well as white matter (WM) and cerebrospinal fluid (CSF) signals, were removed as nuisance variables. WM and CSF masks for this procedure were derived from the tissue segmentation of each subject's T1 scan in native space. Next, functional images were normalized to the MNI space using the echo-planar imaging (EPI) template from SPM (Ashburner and Friston, 1999), and then they were smoothed with an 8-mm full-width half-maximum Gaussian kernel. Finally, data was band-pass filtered (0.01–0.08 Hz) given the relevance of slow frequency in the analysis of resting-state networks (Fox et al., 2005; Raichle, 2009). Then, we compared the mean translational and mean rotational parameters between groups in each country through ANOVA: no differences were found in any of the centers (Table 1).

2.4. Data cleaning

To ensure that algorithms are fed with appropriate training data, and as a complement to the standard pre-processing pipeline described in Section 2.3, we further cleaned the BOLD fMRI time series by despiking the signal with a wavelet-based algorithm (Patel et al., 2014) (Fig. 1. B). This spatially-adaptive, wavelet-based method for identifying, modeling, and removing non-stationary events in fMRI time series caused by head movement is able to accommodate the substantial spatial and temporal heterogeneity of motion artifacts. Therefore, this procedure can remove a range of high- and low-frequency artifacts from fMRI time series, which may be linearly or non-linearly related to physical movements. The Wavelet Despiking algorithm comprises five key steps. First, each voxel time series is decomposed in the wavelet domain. Second, the maximum and minimum wavelet coefficients are defined. Third, the maximum and minimum coefficients of the decomposition are searched, as abrupt changes in time series are represented as chains of maximal and minimal wavelet coefficients. Then, the maximum and minimum coefficients are set to zero. Finally, after the spikes have been removed, the wavelet despiked (denoised) signal is recomposed into the time-series space by using the inverse wavelet transform. Importantly, wavelet denoising yields more robust results than traditional filters, such as time despiking methods (Patel et al., 2014).

2.5. Time series segmentation

Using pre-processed and cleaned BOLD time series as input, we segment the time-series into non-overlapping time windows, reducing its dimensionality while avoiding serial correlations when compared to other segmentation methods (Haimovici et al., 2017) (Fig. 1 C, Supplementary information 3). The aim of this step was to prepare our time-dependent analysis of dynamic connectivity.

2.6. Seed analysis and resting-state network definition

First, seed analysis was used to evaluate both linear and non-linear fMRI connectivity for both SFC and DCFA analyses using the $I\phi^2$ (details below) of five well-known RSNs (Fox et al., 2005): the SN, typically impaired in bvFTD (Sedeño et al., 2017; Sedeño et al., 2016; Agosta et al., 2013); the DMN, characteristically affected in AD (Greicius et al., 2004) but

also compromised in bvFTD (Zhou et al., 2010); the executive network (EN), affected in AD (Agosta et al., 2012) and in bvFTD (Filippi et al., 2019); and the motor network (MN) and the visual network (VN), less markedly compromised in AD (Badhwar et al., 2017) (Fig. 1.D, Supplementary information 4).

2.7. Dependence measure

Dependence measures, such as Mutual Information (MI), capture both linear and non-linear dependencies. Yet, their application in fMRI studies is limited because of their low temporal resolution. MI calculation usually involves the estimation of probability distributions which require a high sample rate to yield adequate results. To overcome this issue, our DCFA analysis used rank statistics in a non-parametric and non-linear dependency measure called the Hoeffding's phi-square ($I\phi^2$, Supplementary information 5) -an approach which circumvents the short-comings of probability estimations.

2.8. Feature engineering and data normalization

After obtaining the masked connectivity RSNs for each time segment, we spatially averaged the voxels of each network within the time segment to obtain a scalar connectivity value for each time segment. Then, we applied the standard deviation statistic to the values of each segment to assess the amount of fluctuation present in the RSN connectivity. Since this approach was employed in each of the segmented time series, considering five different time scales (i.e., 5, 10, 15, 20, and 25 time-points) for five different RSNs (DMN, SN, EN, MN and VN), we obtained a total of 25 features per subject (Fig. 1. E). Then, following feature engineering, we normalized (i.e. z-scored) each patient group (i.e., AD and bvFTD) features by subtracting the mean of the corresponding Control group feature sample and dividing it by its sample standard deviation (Donnelly-Kehoe, 2019). This normalization approach was also employed in the SFC analysis.

2.9. Machine learning classification

For our analysis within Country-1, and in order to obtain an independent test set to evaluate the generalizability of our model, we first split in half the dataset to create a training and testing set. Then, within the training sample, we performed a leave-one-out cross-validation (LOOCV) scheme for hyper-parameter tuning. After the model was trained and cross-validated in this training sample, we evaluated the results in the other half of the data set which is independent from the training set. The following analysis involved training the model with the whole dataset corresponding to Country-1 to predict classification in the other two datasets (from Country-2 and Country-3). We have used the online database as a full out-of-sample validation, having an independent sample not only for testing, but also for training, with the aim to confirm the model's reproducibility from scratch by arriving to the same conclusions starting from different training sets (Saito et al., 2015). Then, we trained the model with the whole dataset corresponding to Country-1 to predict classification in the other two datasets (from Country-2 and Country-3). We then used an independent training and test set from the online database, where each sample (i.e., controls, AD, and bvFTD groups) was divided in two groups, resulting in one half for training and one half for testing. We used a GBM classifier library called XGBoost (eXtreme Gradient Boosting), a classification algorithm employed in fMRI analysis. Compared to other algorithms,

XGBoost proves more robust and is less affected by irrelevant and redundant features (Chang et al., 2019). The algorithm was tuned by Bayesian optimization (Supplementary information 6) (Fig. 1.F).

2.10. Complementary comparisons with structural measures (MRI analysis)

Cortical morphometric features for the machine learning classification were obtained via SBM (Clarkson et al., 2011). This procedure provides regionally specific anatomical metrics, such as volume, curvature, regularity, and cortical thickness. Also, it avoids registration to a standard space, improving the parcellation process and thus offering reliable region-specific metrics to analyze structural changes (Clarkson et al., 2011). All T1 brain volumes were processed accordingly to obtain a complete morphometric description using the FreeSurfer's (v 6.0) image analysis suite (Fischl, 2012). The morphometric procedures of this toolbox show good test-retest reliability across scanner manufacturers and field strengths (Fischl, 2012). Finally, the volume, area, and thickness from each segmentation based on the Desikan-Killiany parcellation of cortical and subcortical areas (Desikan et al., 2006) were quantified to obtain the regional structural features for each subject.

3. Results

3.1. Classification within Country-1

The first analysis comprised the whole dataset from Country-1. Half the participants of each group (controls, AD, and bvFTD patients) were used in the training dataset for hyperparameter tuning with LOOCV validation, and the other half was employed as the testing dataset to measure generalization. The classification accuracy ranking plots (Fig. 2A) show that, for bvFTD against controls, the combination of SN and EN variability features provided the highest classification (accuracy = 83.33%, AUC = 0.91, sensitivity = 80%, specificity = 87.5%). For the AD vs. controls classification, the best features resulted from the combination of the DMN and the EN (accuracy = 86.67%, AUC = 0.90, sensitivity = 83.33%, specificity = 88.89%). Finally, for the bvFTD vs. AD contrast, the best results stemmed from the combination of the SN and the DMN (accuracy = 82.35%, AUC = 0.89, sensitivity = 87.50%, specificity = 71.43%) (Fig. 2–3). All these results were obtained with the 15 time-point window; all other analyses yielded lower results for each classification model (Supplementary information 7).

3.2. Generalization to Country-2 and Country-3

To assess the robustness of our results, we trained with the complete Country-1 dataset and tested in the datasets from the other two countries, featuring different acquisition parameters and sociocultural characteristics. First, we trained with Country-1 data using a LOOCV validation scheme, and tested in the Country-2 dataset. For the bvFTD vs. controls classification, SN and EN variability features provided the highest classification (accuracy = 88.89%, AUC = 0.94, sensitivity = 92.31%, specificity = 89.47%); for AD vs. controls, the combination of the DMN and the EN offered the best classification (accuracy = 89.47%, AUC = 0.88, sensitivity = 94.44%, specificity = 85%); and for the bvFTD vs AD classification, the combination of the SN and the DMN yielded the best results (accuracy = 85.29%, AUC = 0.85, sensitivity = 80%, specificity = 89.47%) (Fig. 2–3). These results

were also obtained under a 15 time-point window. Then, we evaluated classification performance using Country-3 data. For the bvFTD vs. controls, SN and EN variability features provided the highest classification (accuracy = 87.50%, AUC = 0.95, sensitivity = 88.89%, specificity = 85.71%); for AD vs. controls, the combination of the DMN and the EN offered the best results (accuracy = 84.38%, AUC = 0.92, sensitivity = 88.24%, specificity = 80%); and for the bvFTD vs AD classification, the combination of the SN and the DMN offered the highest outcomes (accuracy = 83.87%, AUC = 0.90, sensitivity = 75%, specificity = 93.33%) (Figs. 2, 3). These results were also obtained under the 15 time-point window (Supplementary information 7).

3.3. Classification with the online database

Next, we assessed the generalizability of our method using the online database (Fig. 2A, column 4). For bvFTD vs. controls, SN and EN variability features provided the highest classification (accuracy = 86%, AUC = 0.86, sensitivity = 84.62%, specificity = 87.50%); for AD vs. controls, the highest classification was obtained with a combination of the DMN and the EN (accuracy = 86%, AUC = 0.87, sensitivity = 87.5%, specificity = 84.62%); and for the bvFTD vs AD classification, the highest outcomes were obtained through a combination of the SN and the DMN (accuracy = 80%, AUC = 0.83, sensitivity = 82.61%, specificity = 77.78%) (Figs. 2, 3). These results were also obtained under the 15 time-point window (Supplementary information 7).

3.4. Supplementary analyses results

To compare the performance of our non-linear DCFA with SFC and linear DCFA, we employed the same datasets and the same machine-learning pipeline, obtaining the following results:

3.4.1. Comparison of non-linear DCFA versus SFC—This analysis allowed evaluating whether DCFA outperforms the typical average connectivity analysis (SFC) using the $I\phi^2$ copula dependence method. The DCFA average classification accuracy across datasets was: 86.43% for bvFTD vs. controls, 86.63% for AD vs. controls, and 82.67% for bvFTD vs AD, outperforming SFC (76.66% for bvFTD vs. controls, 76.80% for AD vs. controls, and 76.72% for bvFTD vs AD) (Supplementary information 8).

3.4.2. Comparison of nonlinear DCFA versus linear DCFA analysis—We executed a DCFA but using R instead of the $I\phi^2$ copula dependence measure, to analyze the benefit of considering non-linear associations between brain regions. The resulting average classification accuracy across databases for linear DCFA was: 73.57% for bvFTD vs. controls, 70.74% for AD vs. controls, and 70.22% for bvFTD vs AD -once again, outperformed by nonlinear DCFA (Supplementary information 9).

3.4.3. Comparison of nonlinear DCFA versus T1 atrophy measures—To compare the classification results yielded by connectivity (both DCFA and traditional SFC) with those obtained through brain structural T1 atrophy, we employed non-parametric tests to track statistically significant differences between ROC curves (Venkatraman, 2000) for the two comparisons (i.e., DCFA vs. SFC, and DCFA vs. atrophy). In this approach, the

equality of the curves is analyzed at all operating points, and a reference distribution is generated by permuting the pooled ranks of the test scores for each classification. We found that, although the atrophy-based classification was significantly higher than SFC (Fig. 4A), it was not statistically different from that yielded by DCFA (Fig. 4B).

4. Discussion

Results provide the first non-linear dynamical fluctuations pathophysiological characterization of global RSN in AD and bvFTD across multicentric data. The non-linear DFCA yielded a better classification between controls, AD, and bvFTD across centers compared to canonical connectivity approaches (including both static and linear dynamic connectivity). The classification accuracy ranking showed that the SN-EN pair offered the best classification between bvFTD and controls; whereas the DMN-EN pair provided the highest classification between AD and controls; and the SN-DMN pair offered the best classification between bvFTD and AD. Previous evidence suggests that bvFTD targets the SN, a network responsible for social-emotional-autonomic processing, and networks comprising the executive abilities (Ranasinghe et al., 2016; Ibanez and Manes, 2012; Baez et al., 2014; Baez et al., 2016; Baez et al., 2016; Baez et al., 2016; García-Cordero, 2016; García-Cordero et al., 2015; Ibáñez, 2018; Ibáñez et al., 2017). As regards AD, disruptions of DMN, a network associated with autobiographic memory and hubs affected in AD, have been reported in mild cognitive decline and AD (Grieder et al., 2018), along with EN alterations (Zhao et al., 2018). Our results show that these networks were affected in each condition following the ranking of expected compromise. When comparing bvFTD with AD, divergent network connectivity patterns emerged between the DMN and the SN, consistent with known reciprocal network combinations and the strength and deficit profile of each disorder (Zhou et al., 2010). Moreover, distinct MRI atrophy patterns in regions associated with the DMN and the SN discriminate between these dementias, with a similar anatomical involvement measured as FDG-PET hypometabolism (Foster et al., 2007), and in amyloid ligand Pittsburgh compound B (PiB) (Rabinovici et al., 2011). Here, network combinations afforded higher classification accuracy, suggesting that the pathophysiological profile of specific dementia types involves a distributed pattern of fluctuating RSNs rather than disruptions of a single, static, linear network. The classification accuracy ranking analysis enabled us to weigh each RSN combination, yielding the expected relevance for AD and bvFTD, with other networks (e.g., MN and VN) emerging as noncontributing factors for classification. Higher classification accuracy was obtained when training with the whole Country-1 dataset and testing with the Country-2 and Country-3 datasets, in comparison with training with half Country-1 dataset and testing with the other half. As in the latter case we used a smaller training dataset, subtle differences can be observed in an under-fitting model, thus resulting in (relatively) lower classification scores. Notably, the results of this data-driven approach were consistent despite heterogeneous acquisitions.

Unlike previous methods, our data-driven machine-learning approach showed a disease-specific disturbance of dynamic temporal fluctuations in key RSNs, providing insights into the pathophysiological mechanisms of bvFTD and AD. Previous studies have adopted temporally stationary characterization of the SN in bvFTD (Pievani et al., 2014) and the DMN for AD (Agosta et al., 2012; Greicius et al., 2004). The dynamic temporal nature of

brain activity, as revealed via fMRI time-series fluctuations, should be affected differentially by aging and neurodegeneration. Even while assuming that RSNs are static in the spatial domain, our report taps on brain dynamics using static parcellations of brain networks, as done before (Deco et al., 2017; Tagliazucchi et al., 2012; Glomb et al., 2018; Ipiña, 2020; Stevner et al., 2019). Atypical fluctuations are a basic outcome in neurodegeneration at different levels across different mechanisms (Fornito et al., 2015). Findings suggest pathophysiological fluctuations in neurodegeneration, as already described at different levels, including neuroligins and neurexins, histaminergic, proteome, copper, and metabolic perturbations, as well as white matter, neural synchrony, and global brain dynamics (Filippi et al., 2019). These multilevel mechanisms, from molecular to large-network assemblies, may potentially have an effect on the dynamical network fluctuations of neurodegeneration.

We found that inclusion of FC fluctuations increased classification accuracy for each dementia subtype. Previous studies showed that differences in brain meta-state dwell time, particularly in DMN states, is a hallmark of AD. Decreased global metastability between functional networks indicates that oscillatory patterns are progressively altered over the AD continuum (Demirtas et al., 2017). Notably, there is a decline of DFC fluctuations in aging (Chen et al., 2017), and the disruption of DMN dynamics increases cognitive impairment (Wee et al., 2016). In FTD, diminished fluidity has been shown for transitioning between brain states (Premi et al., 2019). Such switching in everyday life may be associated with the fluctuations of a self-organized DFC system, providing the healthy neural substrate needed for cognitive tasks (Deco and Corbetta, 2011). Computational modelling has shown that FC fluctuations represent a fundamental emergent feature of large-scale dynamics that supports flexible cognition (Deco and Corbetta, 2011). Thus, abnormal transient activity of RSNs may provide relevant information for detecting neurodegeneration.

Traditional DFC analyses using time windows are based on linear correlations. Non-linear relationships have been observed between gray matter atrophy (Gispert et al., 2015) and disease severity. EEG/MEG-derived Synchronization Likelihood (SL) has shown linear and non-linear abnormalities on long-range networks in dementia (Stam et al., 2006). Other non-linear measures based on mutual information have proven robust to better characterize brain networks in FTD (relying on both EEG (Dottori et al., 2017) and fMRI (Moguilner et al., 2018) data). Unlike all these antecedents, in which the measured parameters were fixed for specific contexts, we developed a data-driven pipeline without using any a-priori parameter such as a specific window length or specific RSN disturbance using a Bayesian hyperparameter optimized XGBoost algorithm, enabling us to obtain more generalizable results.

4.1. Relevance for research on disease heterogeneity and diversity

While the classification accuracy ranking of RSNs was similar between measures, higher non-linear DCFA scores were obtained across different groups and datasets (Supplementary information 9 and 10) when compared to linear DCFA and SFC. Multi-centric approaches on diverse populations are needed to find robust and effective biomarkers of global applicability (Sonnen et al., 2008). Population heterogeneity may be underrepresented when local datasets are exclusively employed, especially when using data from high-income

countries[12]. Developing countries have unique interactions between genetics, environmental factors and socioeconomic status (Parra et al., 2018). There is an ongoing need for accurate dementia markers to complement traditional clinical work (Alladi and Hachinski, 2018). Differential diagnosis between AD and bvFTD may prove difficult, as bvFTD could frequently be misdiagnosed as AD, especially in clinical contexts where the costly PET amyloid and CSF markers are not readily available in LMIC (Piguet et al., 2011). Major challenges in neuroradiological protocol design initiatives in LMIC also involve the lack of expertise to perform standardized pre-processing and accurate image interpretation (Schnack et al., 2010; Baez and Ibanez, 2016). Against this background, our data-driven machine learning DCFA pipeline brings a first step to include dynamical networks in the set of complementary, innovative, and affordable tools for decision-support diagnostic tools.

4.2. Limitations and future studies

Our work features some limitations. First, AD and bvFTD diagnoses were based on clinical expertise but without pathological or genetic confirmation. However, the diagnostic criteria for both AD and bvFTD fulfilled standard diagnostic guidelines. This limitation is shared by similar works employing traditional statistical and machine-learning techniques to study dementia (Donnelly-Kehoe, 2019; Zhou et al., 2010). Also, even when the results suggest robust classification despite absent definite diagnosis, future studies may combine confirmative biomarkers to evaluate the effectiveness of neuroimaging metrics. Second, our work focused on functional connectivity, leaving the evaluation of the combination between fMRI and structural (MRI) or metabolic PET imaging for future studies. The objective of this work was to compare the DFCA of functional connectivity fluctuations with traditional seed-based FC measures. Although this excludes multimodal comparisons with atrophy measures, which have been done before (Sedeño et al., 2017; Donnelly-Kehoe, 2019), we performed a complementary analysis with atrophy-based classification outcomes (See Section 3.4, and Fig. 4). While the use of atrophy features provided significantly higher classification results than SFC as previously reported (Sedeño et al., 2017; Donnelly-Kehoe, 2019), these were not significantly different from those obtained through dynamical fluctuation features. Future studies may combine atrophy features with dynamic connectivity as well as other imaging modalities for multimodal classification. While acknowledging the relevance of combining multimodal imaging, the economic constraints in low-income countries may pose difficulties in employing combined or costly biomarker protocols, such as those advanced in the NIA/AA β -Amyloid and pathologic tau PET framework (Jack et al., 2018). However, MR functional methods may be as effective as other biomarkers in providing early diagnosis (Iturria-Medina et al., 2016). Third, no heart rate and respiration measures were available during acquisition, which may have potentially confounded our results if groups differed significantly in this regard. Although this limitation is shared by similar works in neurodegeneration (Grieder et al., 2018; Filippi et al., 2013), further studies should include the physiological rhythms (cardiac rhythm, respiration) as potential features in the machine learning classification. Fourth, although we found a specific set of best performing RSN features as a consistent marker across samples for each classification, we did not systematically assess the statistical significance among all results, as the scope of this work is to generate a data-driven model, rather than performing statistical hypothesis testing. Therefore, we did not prove the statistical significance of the feature within ranking

itself, but we can assess the reproducibility of the results regarding the best performing features across datasets. Lastly, future longitudinal assessments using the present approach may unveil how dynamic network fluctuations unfold over the course of each disease.

5. Conclusions

Although linear, static, averaged FC methods have been proposed as potential biomarkers for neurodegenerative diseases (Pievani et al., 2014), inconsistent results (Zhou et al., 2010; Dopper et al., 2014; Whitwell et al., 2011; Balthazar et al., 2014) and current evidence pointing to dynamical fluctuations in health and disease (Breakspear, 2017; Hutchison et al., 2013) call for a different approach. Our study shows that dynamical brain fluctuations boost dementia classification, providing a data-driven hierarchical model of brain network profiles that mirrors the expected pathophysiological compromise in AD and bvFTD across heterogeneous acquisition contexts. Neural signals continuously combine, dissolve, and reconfigure to produce adaptive patterns of activity over various time scales, producing a repertoire of multi-stable brain states. Our findings provide insights into specific dynamical perturbations of oscillatory brain network architecture in dementias, leading to more plausible biological models, better disease characterization, and, eventually, more targeted drug treatments.

Supplementary Material

Refer to Web version on PubMed Central for supplementary material.

Acknowledgments

We thankfully acknowledge the participation of patients and controls, as well as the support of the patients' families.

Funding

This work is partially supported by grants from CONICET; FONCYT-PICT 2017-1818; FONCYT-PICT 2017-1820; ANID/FONDAP 15150012; Programa Interdisciplinario de Investigación Experimental en Comunicación y Cognición (PIIECC), Facultad de Humanidades, USACH; Alzheimer's Association GBHI ALZ UK-20-639295, and the MULTI-PARTNER CONSORTIUM TO EXPAND DEMENTIA RESEARCH IN LATIN AMERICA [ReDLat, supported by National Institutes of Health, National Institutes of Aging (R01 AG057234), Alzheimer's Association (SG-20-725707), Tau Consortium, and Global Brain Health Institute)]. This work was also supported by ForeFront, a large collaborative research group dedicated to the study of neurodegenerative diseases and funded by the National Health and Medical Research Council of Australia Program Grant (#1132524), Dementia Research Team Grant (#1095127), and the ARC Centre of Excellence in Cognition and its Disorders (CE11000102). OP is supported by a NHMRC Senior Research Fellowship (GNT1103258). FK is supported by a NHMRC Career Development Fellowship (GNT1158762). The contents of this publication are solely the responsibility of the authors and do not represent the official views of these Institutions.

References

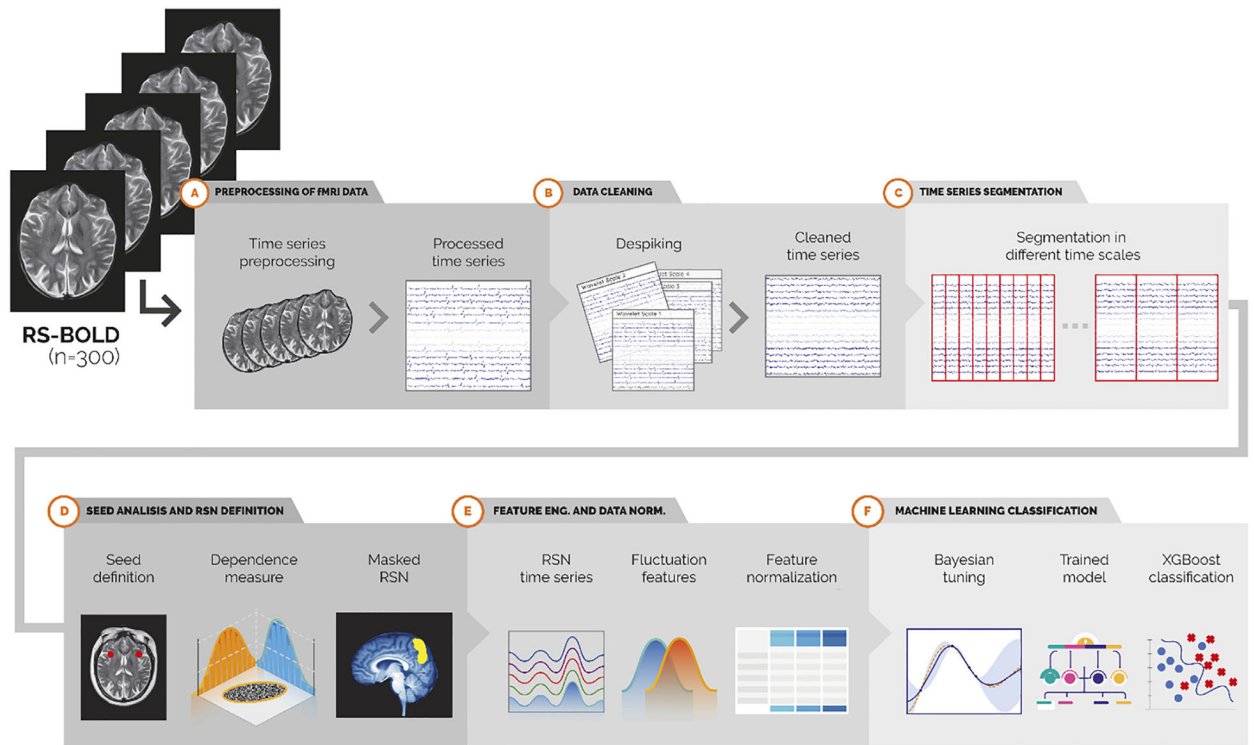
- Agosta F, P. M, Geroldi C, Copetti M, Frisoni GB, Filippi M, 2012 Resting state fMRI in Alzheimer's disease: beyond the default mode network. *Neurobiol Aging*. 33 (8), 1564–1578. [PubMed: 21813210]
- Agosta F, et al., 2013 Brain network connectivity assessed using graph theory in frontotemporal dementia. *Neurology* 81 (2), 134–143. [PubMed: 23719145]
- Alladi S, Hachinski V, 2018 World dementia: one approach does not fit all. *Neurology* 91 (6), 264–270. [PubMed: 29997191]

- Ashburner J, Friston KJ, 1999 Nonlinear spatial normalization using basis functions. *Hum. Brain Mapp* 7 (4), 254–266. [PubMed: 10408769]
- Bachli MB, et al., 2020 Evaluating the reliability of neurocognitive biomarkers of neurodegenerative diseases across countries: a machine learning approach. *Neuroimage* 208, 116456. doi: 10.1016/j.neuroimage.2019.116456. [PubMed: 31841681]
- Badhwar A, et al., 2017 Resting-state network dysfunction in Alzheimer’s disease: a systematic review and meta-analysis. *Alzheimers Dement* 8, 73–85.
- Baez S, Ibanez A, 2016 Dementia in Latin America: an emergent silent Tsunami. *Front. Aging Neurosci* 8, 253. doi: 10.3389/fnagi.2016.00253. [PubMed: 27840605]
- Baez S, et al., 2014a Comparing moral judgments of patients with frontotemporal dementia and frontal stroke. *JAMA Neurol.* 71 (9), 1172–1176. [PubMed: 25047907]
- Baez S, et al., 2014b Comparing moral judgments of patients with frontotemporal dementia and frontal stroke. *JAMA Neurol.* 71 (9), 1172–1176. [PubMed: 25047907]
- Baez S, Garcia AM, Ibanez A, 2016 The social context network model in psychiatric and neurological diseases. *Curr. Top. Behav. Neurosci* 30, 379–396. doi: 10.1007/7854_2016_443.
- Baez S, et al., 2016c Integration of intention and outcome for moral judgment in frontotemporal Dementia: brain structural signatures. *Neurodegener. Dis* 16 (3–4), 206–217. [PubMed: 26859768]
- Baez S, et al., 2016d Orbitofrontal and limbic signatures of empathic concern and intentional harm in the behavioral variant frontotemporal dementia. *Cortex* 75, 20–32. [PubMed: 26707083]
- Baez S, et al., 2019 Brain structural correlates of executive and social cognition profiles in behavioral variant frontotemporal dementia and elderly bipolar disorder. *Neuropsychologia* 126, 159–169. [PubMed: 28219620]
- Baez S, et al., 2016 Integration of intention and outcome for moral judgment in frontotemporal dementia: brain structural signatures. *Neurodegener. Dis* 16, 206–217. doi: 10.1159/000441918. [PubMed: 26859768]
- Balthazar ML, et al., 2014 Neuropsychiatric symptoms in Alzheimer’s disease are related to functional connectivity alterations in the salience network. *Hum. Brain Mapp* 35 (4), 1237–1246. [PubMed: 23418130]
- Bassett DS, et al., 2011 Dynamic reconfiguration of human brain networks during learning. *Proc. Natl. Acad. Sci. U. S. A* 108 (18), 7641–7646. [PubMed: 21502525]
- Bolton TA, Morgenroth E, Preti MG, Van De Ville D, 2020 Tapping into multi-faceted human behavior and psychopathology using fMRI brain dynamics. *Trends Neurosci.* 43 (9), 667–680. [PubMed: 32682563]
- Breakspear M, 2017 Dynamic models of large-scale brain activity. *Nat. Neurosci* 20 (3), 340–352. [PubMed: 28230845]
- Caso F, Cursi M, Magnani G, Fanelli G, Falautano M, Comi G, Leocani L, Minicucci F, 2012 Quantitative EEG and LORETA: valuable tools in discerning FTD from AD? *Neurobiol. Aging* 33 (10), 2343–2356. [PubMed: 22244088]
- Chang C, Glover GH, 2010 Time-frequency dynamics of resting-state brain connectivity measured with fMRI. *Neuroimage* 50 (1), 81–98 2010. [PubMed: 20006716]
- Chang W, Liu Y, Xiao Y, Yuan X, Xu X, Zhang S, Zhou S, 2019 A machine-learning-based prediction method for hypertension outcomes based on medical data. *Diagnostics* 9 (4), 178.
- Chen Y, et al., 2017 Age-related decline in the variation of dynamic functional connectivity: a resting state analysis. *Front. Aging Neurosci* 9, 203. [PubMed: 28713261]
- Clarkson MJ, et al., 2011 A comparison of voxel and surface based cortical thickness estimation methods. *Neuroimage* 57 (3), 856–865. [PubMed: 21640841]
- Deco G, Corbetta M, 2011 The dynamical balance of the brain at rest. *Neuroscientist* 17 (1), 107–123. [PubMed: 21196530]
- Deco G, Kringelbach ML, Jirsa VK, et al., 2017 The dynamics of resting fluctuations in the brain: metastability and its dynamical cortical core. *Sci. Rep* 7, 3095. [PubMed: 28596608]
- Demirtas M, et al., 2017 A whole-brain computational modeling approach to explain the alterations in resting-state functional connectivity during progression of Alzheimer’s disease. *Neuroimage Clin.* 16, 343–354. [PubMed: 28861336]

- Desikan RS, et al., 2006 An automated labeling system for subdividing the human cerebral cortex on MRI scans into gyral based regions of interest. *Neuroimage* 31 (3), 968–980. [PubMed: 16530430]
- Donnelly-Kehoe PA, et al., 2019a Robust automated computational approach for classifying frontotemporal neurodegeneration: multimodal/multicenter neuroimaging. *Alzheimers Dement* 11, 588–598. doi: 10.1016/j.dadm.2019.06.002.
- Donnelly-Kehoe PA, et al., 2019 Robust automated computational approach for classifying frontotemporal neurodegeneration: multimodal/multicenter neuroimaging. *Alzheimers Dement* 11, 588–598. doi: 10.1016/j.dadm.2019.06.002.
- Dopper EG, et al., 2014 Structural and functional brain connectivity in presymptomatic familial frontotemporal dementia. *Neurology* 83 (2), 19–26. [PubMed: 24920855]
- Dottori M, et al., 2017a Towards affordable biomarkers of frontotemporal dementia: a classification study via network’s information sharing. *Sci. Rep* 7 (1), 3822. [PubMed: 28630492]
- Dottori M, et al., 2017b Towards affordable biomarkers of frontotemporal dementia: a classification study via network’s information sharing. *Sci. Rep* 7 (1), 3822. [PubMed: 28630492]
- Filippi M, et al., 2013 Functional network connectivity in the behavioral variant of frontotemporal dementia. *Cortex* 49 (9), 2389–2401. [PubMed: 23164495]
- Filippi M, et al., 2019 Resting state dynamic functional connectivity in neurodegenerative conditions: a review of magnetic resonance imaging findings. *Front. Neurosci* 13, 657. [PubMed: 31281241]
- Fischl B, 2012 FreeSurfer. *Neuroimage* 62 (2), 774–781. [PubMed: 22248573]
- Fornito A, Zalesky A, Breakspear M, 2015 The connectomics of brain disorders. *Nat. Rev. Neurosci* 16 (3), 159–172. [PubMed: 25697159]
- Foster NL, et al., 2007 FDG-PET improves accuracy in distinguishing frontotemporal dementia and Alzheimer’s disease. *Brain* 130 (Pt 10), 2616–2635. [PubMed: 17704526]
- Fox M, et al., 2005 The human brain is intrinsically organized into dynamic, anticorrelated functional networks. *Proc Natl Acad Sci U S A.* 102 (27), 9673–9678. [PubMed: 15976020]
- García-Cordero I, et al., 2015 Stroke and neurodegeneration induce different connectivity aberrations in the Insula. *Stroke* 46 (9), 2673–2677. [PubMed: 26185182]
- García-Cordero I, et al., 2016 Feeling, learning from and being aware of inner states: interoceptive dimensions in neurodegeneration and stroke. *Philos. Trans. R. Soc. Lond. B Biol. Sci* 371 (1708). doi: 10.1098/rstb.2016.0006.
- Garcia-Cordero I, et al., 2019 Explicit and implicit monitoring in neurodegeneration and stroke. *Sci. Rep* 9 (1), 14032. [PubMed: 31575976]
- Gispert JD, et al., 2015 Nonlinear cerebral atrophy patterns across the Alzheimer’s disease continuum: impact of APOE4 genotype. *Neurobiol. Aging* 36 (10), 2687–2701. [PubMed: 26239178]
- Glomb K, et al., 2018 Stereotypical modulations in dynamic functional connectivity explained by changes in BOLD variance. *Neuroimage* 171, 40–54. [PubMed: 29294385]
- Greicius MD, et al., 2004 Default-mode network activity distinguishes Alzheimer’s disease from healthy aging: evidence from functional MRI. *Proc. Natl. Acad. Sci. U. S. A* 101 (13), 4637–4642. [PubMed: 15070770]
- Greicius MD, et al., 2008 Resting-state functional connectivity in neuropsychiatric disorders. *Curr. Opin. Neurol* 21, 424–430. [PubMed: 18607202]
- Grieder M, et al., 2018 Default mode network complexity and cognitive decline in mild Alzheimer’s disease. *Front. Neurosci* 12, 770. [PubMed: 30405347]
- Haimovici A, et al., 2017 On wakefulness fluctuations as a source of BOLD functional connectivity dynamics. *Sci. Rep* 7 (1), 5908. [PubMed: 28724928]
- Handwerker DA, et al., 2012 Periodic changes in fMRI connectivity. *Neuroimage* 63 (3), 1712–1719. [PubMed: 22796990]
- Humpel C, 2011 Identifying and validating biomarkers for Alzheimer’s disease. *Trends Biotechnol.* 29 (1), 26–32. [PubMed: 20971518]
- Hutchison RM, et al., 2013 Dynamic functional connectivity: promise, issues, and interpretations. *Neuroimage* 80, 360–378. [PubMed: 23707587]
- Ibáñez A, et al. 2017 Reply: towards a neurocomputational account of social dysfunction in neurodegenerative disease. *Brain* 140 (3), e15. [PubMed: 27993891]

- Ibáñez A, 2018 Brain oscillations, inhibition and social inappropriateness in frontotemporal degeneration. *Brain* 141 (10), e73. [PubMed: 30212838]
- Ibanez A, Kosik KS, 2020 COVID-19 in older people with cognitive impairment in Latin America. *The Lancet Neurol.* 19 (9), 719–721.
- Ibanez A, Manes F, 2012 Contextual social cognition and the behavioral variant of frontotemporal dementia. *Neurology* 78 (17), 1354–1362. [PubMed: 22529204]
- Ipiña IP, et al., 2020 Modeling regional changes in dynamic stability during sleep and wakefulness. *Neuroimage* 215, 116833. doi: 10.1016/j.neuroimage.2020.116833. [PubMed: 32289454]
- Iturria-Medina Y, et al., 2016 Early role of vascular dysregulation on late-onset Alzheimer's disease based on multifactorial data-driven analysis. *Nat. Commun* 7, 11934. [PubMed: 27327500]
- Jack CR Jr., et al., 2018 NIA-AA Research Framework: toward a biological definition of Alzheimer's disease. *Alzheimers Dement* 14 (4), 535–562. [PubMed: 29653606]
- Kalaria RN, et al., 2008 Alzheimer's disease and vascular dementia in developing countries: prevalence, management, and risk factors. *Lancet Neurol.* 7 (9), 812–826. [PubMed: 18667359]
- Liegeois R, et al., 2019 Resting brain dynamics at different timescales capture distinct aspects of human behavior. *Nat. Commun* 10 (1), 2317. [PubMed: 31127095]
- Melloni M, et al., 2016 Your perspective and my benefit: multiple lesion models of self-other integration strategies during social bargaining. *Brain* 139 (11), 3022–3040. doi: 10.1093/brain/aww231. [PubMed: 27679483]
- Moguilner S, et al., 2018 Weighted Symbolic Dependence Metric (wSDM) for fMRI resting-state connectivity: a multicentric validation for frontotemporal dementia. *Sci. Rep* 8 (1), 11181. [PubMed: 30046142]
- Noh Y, et al., 2014 Anatomical heterogeneity of Alzheimer disease: based on cortical thickness on MRIs. *Neurology* 83 (21), 1936–1944. [PubMed: 25344382]
- Ossenkopppele R, et al., 2015 The behavioural/dysexecutive variant of Alzheimer's disease: clinical, neuroimaging and pathological features. *Brain* 138 (Pt 9), 2732–2749. [PubMed: 26141491]
- Parra MA, et al., 2018 Dementia in Latin America: assessing the present and envisioning the future. *Neurology* 90 (5), 222–231. [PubMed: 29305437]
- Parra M, et al., 2020 Dementia in Latin America: Paving the way towards a regional action plan. *Alzheimers & Dementia* doi: 10.1002/alz.12202.
- Patel AX, Kundu P, Rubinov M, Jones PS, Vértes PE, Ersche KD, Suckling J, Bullmore ET, 2014 A wavelet method for modeling and despiking motion artifacts from resting-state fMRI time series. *Neuroimage* 95 (100), 287–304. [PubMed: 24657353]
- Pievani M, et al., 2014 Brain connectivity in neurodegenerative diseases—from phenotype to proteinopathy. *Nat. Rev. Neurol* 10 (11), 620–633. [PubMed: 25287597]
- Piguet O, et al., 2011a Eating and hypothalamus changes in behavioral-variant frontotemporal dementia. *Ann. Neurol* 69 (2), 312–319. [PubMed: 21387376]
- Piguet O, et al., 2011b Behavioural-variant frontotemporal dementia: diagnosis, clinical staging, and management. *Lancet Neurol.* 10 (2), 162–172. [PubMed: 21147039]
- Poldrack RA, et al., 2017 Scanning the horizon: towards transparent and reproducible neuroimaging research. *Nat. Rev. Neurosci* 18 (2), 115–126. [PubMed: 28053326]
- Premi E, et al., 2019 The inner fluctuations of the brain in presymptomatic Frontotemporal Dementia: the chronnectome fingerprint. *Neuroimage* 189, 645–654. [PubMed: 30716457]
- Rabinovici GD, R. H, Alkalay A, Kornak J, Furst AJ, Agarwal N, Mormino EC, O'Neil JP, Janabi M, Karydas A, Growdon ME, Jang JY, Huang EJ, Dearmond SJ, Trojanowski JQ, Grinberg LT, Gorno-Tempini ML, Seeley WW, Miller BL, Jagust WJ, 2011 Amyloid vs FDG-PET in the differential diagnosis of AD and FTL. *Neurology* 77 (23), 2034–2042. [PubMed: 22131541]
- Raichle ME, 2009 A paradigm shift in functional brain imaging. *J. Neurosci* 29 (41), 12729–12734. [PubMed: 19828783]
- Ranasinghe KG, et al., 2016 Distinct subtypes of behavioral variant frontotemporal Dementia based on patterns of network degeneration. *JAMA Neurol.* 73 (9), 1078–1088. [PubMed: 27429218]
- Saito PT, Nakamura RY, Amorim WP, Papa JP, de Rezende PJ, Falcão AX, 2015 Choosing the most effective pattern classification model under learning-time constraint. *PLoS One* 10 (6).

- Santamaria-Garcia H, et al., 2017 A lesion model of envy and Schadenfreude: legal, deservingness and moral dimensions as revealed by neurodegeneration. *Brain* 140 (12), 3357–3377. [PubMed: 29112719]
- Schnack HG, et al., 2010 Mapping reliability in multicenter MRI: voxel-based morphometry and cortical thickness. *Hum. Brain Mapp* 31 (12), 1967–1982. [PubMed: 21086550]
- Sedeño L, et al., 2016 Brain network organization and social executive performance in frontotemporal Dementia. *J. Int. Neuropsychol. Soc* 22 (2), 250–262. [PubMed: 26888621]
- Sedeño L, et al., 2017 Tackling variability: a multicenter study to provide a gold-standard network approach for frontotemporal dementia. *Hum Brain Mapp*. 3804–3822. doi: 10.1002/hbm.23627. [PubMed: 28474365]
- Shakil S, Lee CH, Keilholz SD, 2016 Evaluation of sliding window correlation performance for characterizing dynamic functional connectivity and brain states. *Neuroimage* 133, 111–128. [PubMed: 26952197]
- Sonnen JA, et al., 2008 Biomarkers for cognitive impairment and dementia in elderly people. *Lancet Neurol*. 7 (8), 704–714. [PubMed: 18635019]
- Sporns O, 2014 Contributions and challenges for network models in cognitive neuroscience. *Nat. Neurosci* 17 (5), 652–660. [PubMed: 24686784]
- Stam CJ, et al., 2006 Magnetoencephalographic evaluation of resting-state functional connectivity in Alzheimer’s disease. *Neuroimage* 32 (3), 1335–1344. [PubMed: 16815039]
- Stevner ABA, et al., 2019 Discovery of key whole-brain transitions and dynamics during human wakefulness and non-REM sleep. *Nat. Commun* 10 (1), 1035. [PubMed: 30833560]
- Tagliazucchi E, et al., 2012a Dynamic BOLD functional connectivity in humans and its electrophysiological correlates. *Front. Hum. Neurosci* 6, 339. [PubMed: 23293596]
- Tagliazucchi E, von Wegner F, Morzelewski A, Brodbeck V, Laufs H, 2012b Dynamic BOLD functional connectivity in humans and its electrophysiological correlates. *Front. Hum. Neurosci* 6 (339).
- Venkatraman ES, 2000 A permutation test to compare receiver operating characteristic curves. *Biometrics* 56 (4), 1134–1138. [PubMed: 11129471]
- Wee CY, et al., 2016 Sparse temporally dynamic resting-state functional connectivity networks for early MCI identification. *Brain Imaging Behav*. 10 (2), 342–356. [PubMed: 26123390]
- Whitwell JL, et al., 2009 Distinct anatomical subtypes of the behavioural variant of frontotemporal dementia: a cluster analysis study. *Brain* 132 (Pt 11), 2932–2946. [PubMed: 19762452]
- Whitwell JL, et al., 2011 Altered functional connectivity in asymptomatic MAPT subjects: a comparison to bvFTD. *Neurology* 77 (9), 866–874. [PubMed: 21849646]
- Wu YT, et al., 2017 The changing prevalence and incidence of dementia over time - current evidence. *Nat. Rev. Neurol* 13 (6), 327–339. [PubMed: 28497805]
- Yaesoubi M, Allen EA, Miller RL, Calhoun VD, 2015 Dynamic coherence analysis of resting fMRI data to jointly capture state-based phase, frequency, and time-domain information. *Neuroimage* 120 (133–142).
- Zhao Q, et al., 2018 Evaluating functional connectivity of executive control network and frontoparietal network in Alzheimer’s disease. *Brain Res*. 1678, 262–272. [PubMed: 29079506]
- Zhou J, et al., 2010 Divergent network connectivity changes in behavioural variant frontotemporal dementia and Alzheimer’s disease. *Brain* 133 (Pt 5), 1352–1367. [PubMed: 20410145]

**Fig. 1.**

Preprocessing and machine learning pipeline. **(A)** In order for the RS-BOLD data from the two groups to be classified, we employed the DPARSF pipeline for RS-fMRI data preprocessing, followed by band-pass filtering (0.01–0.08 Hz) to obtain the preprocessed time-series. **(B)** By using a wavelet-based algorithm, we employed the wavelet coefficients to remove large signal spikes without losing relevant information to obtain the cleaned time series. **(C)** We segmented the RS time series into non-overlapping windows of different time-scales (i.e., 5, 10, 15, 20 and 25 time-points). **(D)** We defined seeds for the DMN, SN, EN, VN, and MN networks to obtain the RSNs by employing the $I\phi^2$ copula dependence measure. Then we used standard masks to identify the voxels for each network. **(E)** We spatially averaged the voxels to obtain one RSNs time series for each network. Then we used the standard deviation statistic to obtain the fluctuation features for later normalization. **(F)** For testing different feature combinations, we used a LOOCV validation scheme for Bayesian hyper-parameter tuning to obtain trained XGBoost models, and then we tested our classification with independent datasets. For ROC analysis, we defined bvFTD group as the “positive” class and AD group as the “negative” class, allowing the sensitivity and specificity metrics being applicable to patients groups comparisons, as reported previously (Caso et al., 2012). RS-BOLD: fMRI resting-state BOLD datasets; masked RSNs: masked resting-state networks; FEATURE ENG: Feature engineering; DATA NORM: Data normalization.

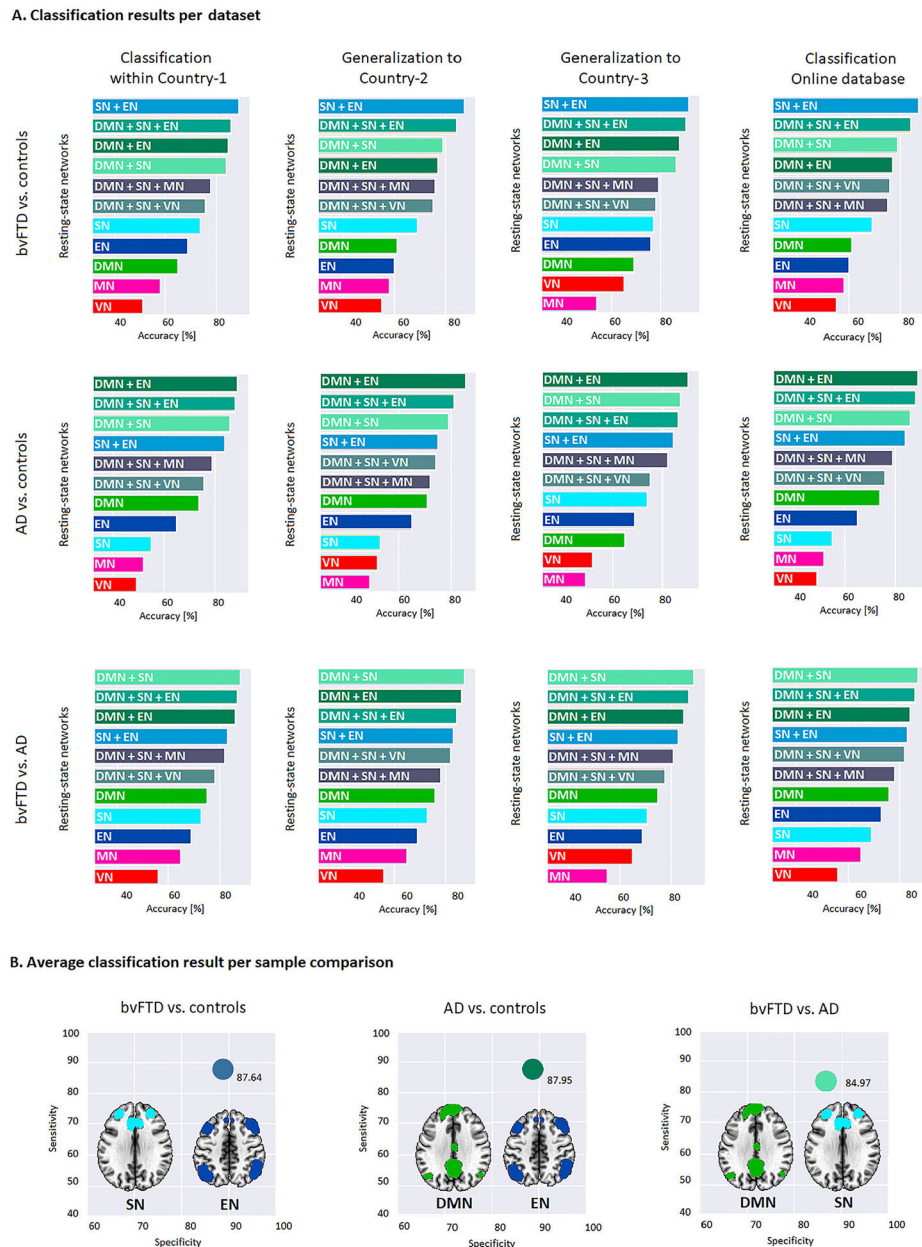


Fig. 2. Classification accuracy rankings and average results. Classification accuracy ranking and average results. **(A)** Binary classification results for bvFTD vs. controls, AD vs. controls, and bvFTD vs. controls, training and testing within Country-1 (first column), training with Country-1 and testing with Country-2 (Generalization to Country 2, second column), training with Country-1 and testing with Country-3 (Generalization to Country-3, third column), and the results from the training and testing of our model with an online databases (ADNI and NIFD, fourth column). Classification accuracy ranking ordered from highest to lowest accuracy rates shows the best set of features for each classification. **(B)** Average results for each classification type over the four analyses showing mean sensitivity (y-axis), specificity (x-axis) and accuracy (average classification accuracy across databases: 87.64%

for bvFTD vs. controls, 87.95% for AD vs. controls, and 84.97% for bvFTD vs AD). C: Healthy control; bvFTD: behavioral-variant frontotemporal dementia; AD: Alzheimer's disease; SN: salience network; EN: executive network; DMN: default mode network; VN: visual network; MN: motor network.

Author Manuscript

Author Manuscript

Author Manuscript

Author Manuscript

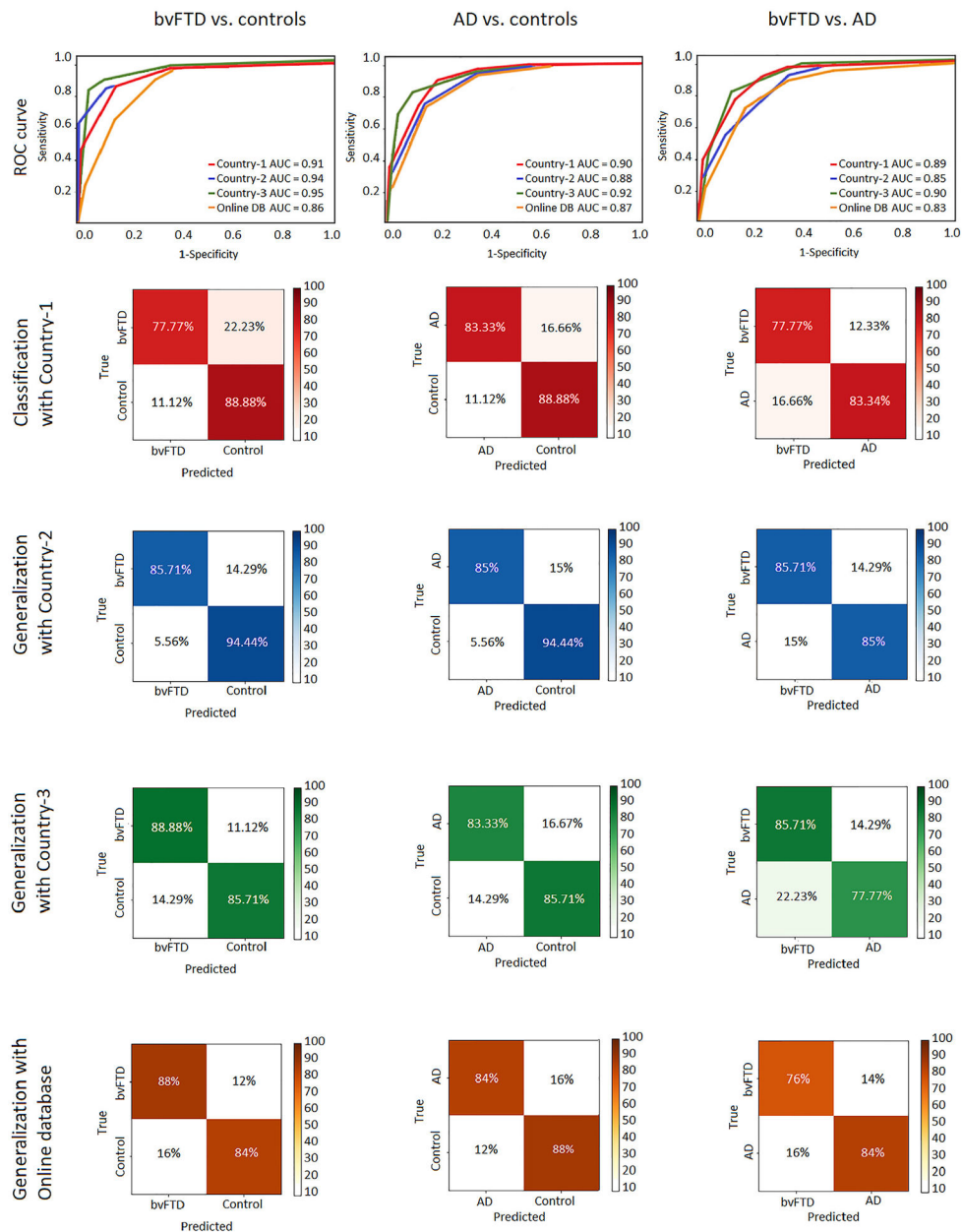
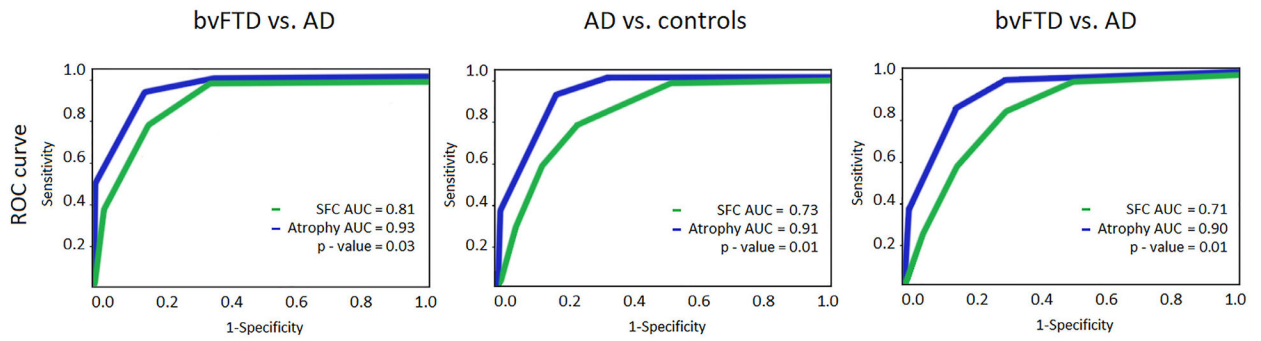


Fig. 3. ROC curves and confusion matrices. First row: Each ROC curve represents the performance of the best resting-state networks for each binary classification model per country (SN + EN networks for bvFTD vs controls; DMN + EN networks for AD vs controls; and DMN + SN for bvFTD vs AD). Second to fifth rows: confusion matrices for each of the ROC curves of the first row (in percentage values). Controls: Healthy control; bvFTD: behavioral variant frontotemporal dementia; AD: Alzheimer's disease; SN: salience network; EN: executive network; DMN: default mode network.

A. SFC vs Atrophy



B. DCFA vs Atrophy

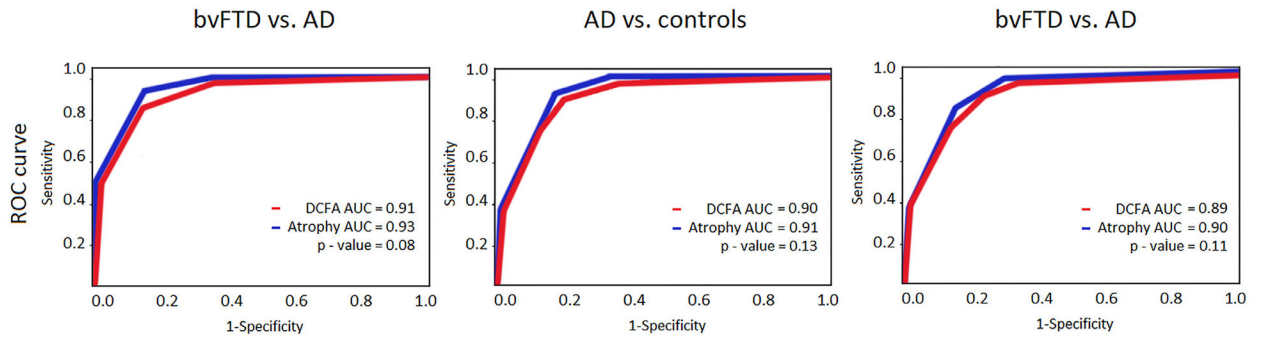


Fig. 4.

Statistical comparison of ROC curves. (A) ROC curves representing the classification performance for Country-1 for each classification pair, with their corresponding AUC value. In green, we show the ROC curve of the SFC classification using the best performing features for the classification (SN + EN networks for bvFTD vs controls; DMN + EN networks for AD vs controls; and DMN + SN for bvFTD vs AD). In blue, we present atrophy AUC results obtained from the classification based on the SBM analysis for each subject. To compare the classification results between the two methodologies, we employed a non-parametric permutation comparison test of the ROC curves (Venkatraman, 2000). All p -values < 0.05 show that there are statistically significant differences between methods for all classification pairs. (B) ROC curves representing the classification performance for Country-1 for each classification pair, with their corresponding AUC value. The ROC curve of the DCFA classification using the best performing features for the classification (SN + EN networks for bvFTD vs controls; DMN + EN networks for AD vs controls; and DMN + SN for bvFTD vs AD) is shown in red. Atrophy measures are plotted in blue. All p -values > 0.05 show significant differences for A (SFC vs atrophy). But not for B (DCFA vs atrophy) in each classification pair.

Table 1

Movement parameters.

	Country-1				Country-2				Country-3				Online database							
	C	bvFTD	AD	Stats Score	p- value	C	bvFTD	AD	Stats Score	p- value	C	bvFTD	AD	Stats Score	p- value	C	bvFTD	AD	Stats Score	p- value
Mean translational (mm)	0.13 (0.02)	0.11 (0.05)	0.10 (0.02)	1.29	.25	0.07 (0.03)	0.06 (0.02)	0.05 (0.02)	1.28	.18	0.08 (0.03)	0.08 (0.03)	0.09 (0.05)	1.61	.22	0.07 (0.02)	0.08 (0.03)	0.07 (0.04)	1.59	.24
Mean rotational (°)	0.08 (0.06)	0.10 (0.03)	0.08 (0.02)	2.99	.12	0.03 (0.01)	0.03 (0.01)	0.05 (0.02)	2.45	.11	0.05 (0.01)	0.03 (0.01)	0.06 (0.03)	3.01	.18	0.04 (0.02)	0.04 (0.04)	0.09 (0.02)	3.2	.09

C: Healthy control.

bvFTD: behavioral variant frontotemporal dementia.

AD: Alzheimer's disease.

Mean (SD).